MOX–Report No. 24/2010

An Uzawa iterative scheme for the simulation of floating boats

LORENZO TAMELLINI, LUCA FORMAGGIA
EDIE MIGLIO, ANNA SCOTTI

MOX, Dipartimento di Matematica "F. Brioschi"
Politecnico di Milano, Via Bonardi 9 - 20133 Milano (Italy)

mox@mate.polimi.it http://mox.polimi.it

An Uzawa iterative scheme for the simulation of floating boats *

Lorenzo Tamellini♯, Luca Formaggia♯, Edie Miglio♯, Anna Scotti♯

July 5, 2010

♯ MOX– Modellistica e Calcolo Scientifico
Dipartimento di Matematica "F. Brioschi"
Politecnico di Milano
via Bonardi 9, 20133 Milano, Italy
lorenzo.tamellini@mail.polimi.it, luca.formaggia@polimi.it,
edie.miglio@polimi.it, anna.scotti@mail.polimi.it

Keywords: Floating body, Free surface flow, Inequality constrained optimization, Uzawa method, Algebraic splitting scheme, Finite elements

AMS Subject Classification: 65K15,76M10, 76M30

Abstract

The numerical simulation of a floating boat requires to solve a complex interaction between free surface flow and the dynamics of the boat. In this work we focus on solution schemes with an explicit representation of the fluid surface and on the specific problem of the imposition of the presence of a floating object. The floating object represents an unilateral constraint on the fluid surface, which cannot rise above a the level defined by the floating object itself. We propose an Uzawa type iterative scheme for this type of situations and we describe an efficient implementation in the context of a particular finite element discretization and algebraic splitting procedure.

Introduction

The dynamics of a floating object like a boat involves a complex interaction between the free surface flow and the intrinsic boat dynamics, the latter being usually described as a rigid body motion.

*This work has been prompted by a collaboration with Filippi Lido srl. The last three authors acknowledge also the support of the Italian Ministry of Research, through PRIN 2007 and PRIN 2008 grants.

In this field, simulations are often performed by adopting the Reynolds Averaged Navier-Stokes (RANS) equations and Volume of Fluid (VOF) or similar techniques [1, 2], where the free surface is captured as the interface between two fluids, air and water. Special procedures and a good mesh refinement are required to obtain a sharp interface, further increasing the already high computational cost of this approach.

To reduce the computational cost, simplified models have been proposed for the study of the dynamics of rowing boats, which is the main target application of the present work. In [3] the hydrodynamic problem is reduced to a complex potential equation for the gravity waves radiated from the boat surface. Viscous effects are accounted for by empirical formulae. This approach provides a very efficient tool at the price of great simplifications on the hydrodynamics.

A different approach is possible when using models where the free surface is described explicitly as a function η for the water elevation. Indeed, the presence of the floating object may be introduced as a constraint on η, which cannot rise above the external surface of the body (suitably extended to cover the region of interest). This point of view permits to exploit efficient schemes for the simulaton of free surface flow in shallow basins, like those developed in [4] and formerly applied mostly to environmental problems. A main limitation of the approach is that the wave cannot overturn, since it is described by a function. However, this limitation is not relevant for a large class of applications, including the one of our concern.

The general technique has been briefly presented already in [5]. In this work we give more details on the derivation of the model and on the numerical scheme used for its solution. We start the first Section by justifying the way we impose the constraint using classic variational arguments. We then specialize the model to the problem at hand. A key ingredient to the the efficient numerical implementation is the characteristic treatment of the time derivative, described in Section 2, which provides an unconditionally stable time advancing scheme. At each time step a weak formulation of the constrained equation is derived and justified, then in Section 3 we present a scheme for its solution based on Uzawa iterations. Another important key to an efficient numerical solution is the splitting of hydrostatic and hydrodynamic pressure. This leads to a fractional step scheme similar to the Chorin-Temam method. The advantage is that the constraint on water elevation is resolved only at the predictor step. This splitting, together with the finite elements used for the space discretization, is described in Section 4. Finally, in Section 5 we provide some numerical results which show the effectiveness of the proposed method.

1 The derivation of the model

Let us first introduce some of the notation that will be used throughout the paper, and recall the basic derivation of the flow equations with no constraints on the free surface.

We consider a fluid filling at each time $t \in (0, T)$ a domain of the form

$$\Omega(t) = \{(x, y, z) : \ (x, y) \in \omega, \ -h < z < \eta(x, y, t)\}, \tag{1}$$

where $\omega \subset \mathbb{R}^2$ is a bounded, regular domain, $h > 0$ is the basin depth, which we assume to be constant.

With $\eta : \omega \times [0, T] \to \mathbb{R}$ we indicate the elevation of the free surface. We also define the following portions of $\partial\Omega(t)$,

$$\Gamma_b = \{(x, y, z) : \ (x, y) \in \omega, \ z = -h\}, \tag{2}$$

$$\Gamma_l = \Gamma_l(t) = \{(x, y, z) : \ (x, y) \in \partial\omega, \ -h < z < \eta(x, y, t)\}, \tag{3}$$

and

$$\Gamma_s = \Gamma_s(t) = \{(x, y, z) : \ (x, y) \in \omega, \ z = \eta(x, y, t)\}. \tag{4}$$

We will address them as bottom, lateral and free surface, respectively. We indicate with $\boldsymbol{U} = (\boldsymbol{u}, w) = (u_x, u_y, w)$ the fluid velocity, where we have put into evidence the horizontal components $\boldsymbol{u}$ and the vertical component w, while Π indicates the fluid pressure. It is understood that they are functions of space and time.

The free surface elevation obeys at any time the following kinematic condition,

$$\frac{D\eta}{Dt} = w \Rightarrow \frac{\partial\eta}{\partial t} + (\boldsymbol{u} \cdot \boldsymbol{\nabla})\eta - w = 0, \quad \text{on } \Gamma_s(t). \tag{5}$$

We assume that the density of the fluid ρ is constant, thus the continuity equation gives

$$\nabla\cdot\boldsymbol{U} = \nabla\cdot\boldsymbol{u} + \frac{\partial w}{\partial z} = 0 \quad \text{in } \Omega(t). \tag{6}$$

Here and in the later sections of the paper we use the same symbols $\boldsymbol{\nabla}$ and $\nabla\cdot$ to indicate the gradient and divergence operators in $\mathbb{R}^3$ as well as those in $\mathbb{R}^2$, depending on the context, with the understanding that they act on the corresponding space variables and vector components.

Finally, we consider the following conditions,

$$\boldsymbol{U} \cdot \boldsymbol{N} = 0 \quad \text{on } \Gamma_l(t) \tag{7}$$

where $\boldsymbol{N} = (\boldsymbol{n}, n_z)$ is the outward normal to $\partial\Omega(t)$ (slip condition), and

$$\boldsymbol{U} = \boldsymbol{0} \quad \text{on } \Gamma_b. \tag{8}$$

Other choices on Γ_b are possible and will be mentioned later.

The D'Alambert-Lagrange variational principle states that the fluid motion obeys at any time the following equation,

$$\int_{\Omega(t)} \rho\boldsymbol{A} \cdot \boldsymbol{\delta P}\, d\Omega + \int_{\Omega(t)} \boldsymbol{\sigma} : \boldsymbol{\nabla}\boldsymbol{\delta P}\, d\Omega - \int_{\Omega(t)} \Pi\nabla\cdot\boldsymbol{\delta P}\, d\Omega - \int_{\partial\Omega(t)} \boldsymbol{t} \cdot \boldsymbol{\delta P}\, d\gamma = \int_{\Omega(t)} \boldsymbol{f} \cdot \boldsymbol{\delta P}\, d\Omega. \tag{9}$$

Here, $\boldsymbol{A} = \dfrac{\partial \boldsymbol{U}}{\partial t} + (\boldsymbol{U} \cdot \boldsymbol{\nabla})\boldsymbol{U}$ is the fluid acceleration, $\boldsymbol{\sigma}$ indicates the viscous part of the Cauchy stress tensor, $\boldsymbol{t}$ and $\boldsymbol{f}$ are the surface stress and external volume force, respectively, while $\boldsymbol{\delta P}$ is any allowable virtual displacement of a fluid particle [6].

The constraints (8) and (7) impose that $\boldsymbol{\delta P} = \boldsymbol{0}$ on Γ_b and $\boldsymbol{\delta P} \cdot \boldsymbol{N} = 0$ on Γ_l. In the following we take $\boldsymbol{f} = \rho \boldsymbol{g}$, where $\boldsymbol{g} = (0, 0, -g)$ is the gravitational acceleration vector, of modulus g. It is well known that (9) is equivalent to the momentum equation

$$\rho \frac{D\boldsymbol{U}}{Dt} - \boldsymbol{\nabla} \cdot \boldsymbol{\sigma} + \boldsymbol{\nabla}\Pi = \rho \boldsymbol{g} \quad \text{in } \Omega(t), \tag{10}$$

complemented with relation $\boldsymbol{\sigma N} - \Pi \boldsymbol{N} = \boldsymbol{t}$ on $\partial\Omega(t)$. The latter, together with the stated conditions on $\boldsymbol{\delta P}$, implies that natural boundary conditions must be applied on the tangential component of the stress on Γ_b and on the whole stress on $\Gamma_s(t)$. We choose here the following relations,

$$\boldsymbol{\sigma N} - \Pi \boldsymbol{N} = -\Pi_a \boldsymbol{N} + \boldsymbol{W} \quad \text{on } \Gamma_s(t) \tag{11}$$

and

$$\boldsymbol{T}_1 \cdot \boldsymbol{\sigma N} = \boldsymbol{T}_2 \cdot \boldsymbol{\sigma N} = 0 \quad \text{on } \Gamma_l(t), \tag{12}$$

where Π_a is a constant reference pressure, $\boldsymbol{W}$ defines the tangential stresses, possibly a given function of $\boldsymbol{U}$, which accounts of external factors like the wind. We have that $\boldsymbol{W} \cdot \boldsymbol{N} = 0$, while $\boldsymbol{T}_1$ and $\boldsymbol{T}_2$ indicate any two linearly independent vectors tangent to Γ_l.

Equations (10) and (6) form the well known Navier-Stokes equations, complemented with boundary conditions (7), (12), (8) and (11). Their solution requires to set an initial condition on the velocity $\boldsymbol{U}$ at time $t = 0$.

1.1 The addition of the constraint

We now consider what happens when we add a unilateral constraint on the surface elevation. More precisely, we impose that at any $t \in (0, T)$

$$\eta \leq \Psi, \quad \text{in } \omega, \tag{13}$$

where $\Psi : \omega \times [0, T] \to \mathbb{R}$ is a given function that represents the position of the floating body. We also make the following

Assumption 1. *At any time $t \in (0, T)$ the set*

$$\gamma_\Psi(t) = \{(x, y) \in \omega : \ \eta(x, y, t) = \Psi(x, y, t)\}$$

satisfies $\gamma_\Psi(t) \subset\subset \omega$.

We also set $\Gamma_\Psi(t) = \{(x,y,z) : (x,y) \in \gamma_\Psi(t),\, z = \eta(x,y,t)\}$. Clearly, thanks to the given assumption, $\Gamma_\Psi(t) \subset\subset \Gamma_s(t)$ during the motion.

To handle this unilateral constraint we introduce a Lagrange multiplier $\lambda : \omega \times (0,T) \to \mathbb{R}$ which satisfies at any time

$$\lambda \geq 0, \qquad \lambda(\eta - \Psi) = 0, \quad \text{in } \omega, \tag{14}$$

and we add to the left hand side of (9) the term

$$-\int_{\Gamma_s} \rho\lambda \boldsymbol{N} \cdot \boldsymbol{\delta P} d\gamma, \tag{15}$$

to represent the virtual work associated with the action that enforces the constraint. We may note that the integral is effectively computed on Γ_Ψ. We note also that on Γ_s the normal vector satisfies the relation

$$\boldsymbol{N} = \kappa^{-1}\left(-\frac{\partial\eta}{\partial x}, -\frac{\partial\eta}{\partial y}, 1\right)^T,$$

with $\kappa = \sqrt{|\boldsymbol{\nabla}\eta|^2 + 1}$, while, thanks to (5), $\delta\eta = -(\delta P_x, \delta P_y) \cdot \boldsymbol{\nabla}\eta + \delta P_z$ is the change of η at a given point (x,y) associated to the virtual displacement $\boldsymbol{\delta P}$. Thus, the integral in (15) is in fact equivalent to $\int_\omega \rho\lambda\delta\eta\, dxdy$, which makes more evident the nature of λ as a Lagrange multiplier associated to constraint (13). The addition of the term (15) to the left hand side of (9) has the consequence that in the differential setting the natural boundary condition on Γ_s changes from (11) to

$$\boldsymbol{\sigma N} - \Pi \boldsymbol{N} = -\Pi_a \boldsymbol{N} + \boldsymbol{W} - \rho\lambda\boldsymbol{N}. \tag{16}$$

It is then convenient to introduce the following change of variable,

$$\Pi = \rho q + \rho g(\eta - z) + \rho\lambda + \Pi_a, \tag{17}$$

where q is called the *hydrodynamic pressure*. The Navier-Stokes problem with constraints becomes

$$\left.\begin{array}{l} \dfrac{D\boldsymbol{U}}{Dt} - \rho^{-1}\boldsymbol{\nabla}\cdot\boldsymbol{\sigma} + \boldsymbol{\nabla}q + g\widetilde{\boldsymbol{\nabla}}\eta + \widetilde{\boldsymbol{\nabla}}\lambda = \boldsymbol{0} \\ \nabla\cdot\boldsymbol{U} = 0 \end{array}\right. \text{ in } \Omega(t), \tag{18}$$

where $\widetilde{\boldsymbol{\nabla}} = (\frac{\partial}{\partial x}, \frac{\partial}{\partial y}, 0)^T$. Furthermore the following relations must hold on ω,

$$\eta - \Psi \leq 0, \quad \lambda \geq 0, \quad \lambda(\eta - \Psi) = 0,$$

and the boundary conditions read,

$$\begin{array}{ll} \boldsymbol{U} = \boldsymbol{0} & \text{on } \Gamma_b, \\ \boldsymbol{U}\cdot\boldsymbol{N} = \boldsymbol{T}_1\cdot\boldsymbol{\sigma N} = \boldsymbol{T}_2\cdot\boldsymbol{\sigma N} = 0 & \text{on } \Gamma_l(t), \\ \rho^{-1}\boldsymbol{\sigma N} - q\boldsymbol{N} + \rho^{-1}\boldsymbol{W} = \boldsymbol{0} & \text{on } \Gamma_s(t). \end{array} \tag{19}$$

This set of equations will form the starting point of our analysis.

We remark that with this model we are in fact assuming a simple impenetrability condition (slip condition) on $\Gamma_\Psi(t)$. Indeed from the kinematic relation for η and the definition of $\boldsymbol{N}$ we have $\boldsymbol{U} \cdot \boldsymbol{N} = \frac{\partial \eta}{\partial t} \boldsymbol{e}_z \cdot \boldsymbol{N}$, $\boldsymbol{e}_z$ being the z-coordinate Cartesian versor, while no a-priori restriction is imposed on the tangential component of the velocity. In the case of viscous fluids it would appear that a no-slip condition that imposes the equality of the fluid velocity with that of the floating surface be more sound from a physical point of view. However, it is well known that this condition is incompatible with a correct evolution of $\Gamma_\Psi(t)$. Nevertheless, with our model we may partially account for the viscous effects by setting $\boldsymbol{W}$ as

$$\boldsymbol{W} = \begin{cases} \boldsymbol{W}_1 & \text{on } \Gamma_s(t) \setminus \Gamma_\Psi(t) \\ \boldsymbol{W}_2 & \text{on } \Gamma_\Psi(t) \end{cases} \tag{20}$$

where $\boldsymbol{W}_1$ accounts for the possible action of the wind on the part of the free surface not in contact with the body, while $\boldsymbol{W}_2 = \boldsymbol{W}_2(\boldsymbol{U})$ may account for the viscous effects as a friction term. In this work, however, we have simply set $\boldsymbol{W} = \boldsymbol{0}$ on the whole $\Gamma_s(t)$, thus effectively using a slip condition on $\Gamma_\Psi(t)$ and assuming no wind action, yet for the sake of completeness we will continue to indicate $\boldsymbol{W}$ in our formulation.

1.2 Specialising the model

It is well known that for a Newtonian incompressible fluid $\boldsymbol{\sigma} = \underline{\underline{\mu}} \left(\boldsymbol{\nabla} \boldsymbol{U} + \boldsymbol{\nabla} \boldsymbol{U}^T \right)$, where $\underline{\underline{\mu}}$ is the dynamic viscosity tensor accounting for different viscosity coefficients in the horizontal (denoted by μ_h) and vertical direction (μ_v) (for further details see [7, 8]).

This in turn implies that the term $\rho^{-1} \boldsymbol{\nabla} \cdot \boldsymbol{\sigma}$ in (18) is equivalent to $\boldsymbol{\nabla} \cdot \left[\underline{\underline{\nu}} \left(\boldsymbol{\nabla} \boldsymbol{U} + \boldsymbol{\nabla} \boldsymbol{U}^T \right) \right]$, where $\underline{\underline{\nu}} = \frac{1}{\rho} \underline{\underline{\mu}}$ is the kinematic viscosity tensor.

However, in our model we neglect the horizontal components of this term and consider only the vertical term $\dfrac{\partial}{\partial z} \left(\nu \dfrac{\partial \boldsymbol{U}}{\partial z} \right)$ (where for the sake of simplicity, from now on, ν will denote the kinematic viscosity in the vertical direction). This is a common choice in hydrodynamic calculations in relatively shallow basins, like the one of our interest [9, 10], and it allows to adopt efficient numerical schemes, as the one detailed later. However, we wish to point out that the analysis and the techniques for the imposition of the constraint illustrated in this paper extend directly to the general case.

As a consequence, the condition on the free surface $\Gamma_s(t)$ becomes

$$\nu \frac{\partial \boldsymbol{U}}{\partial z} - q \boldsymbol{N} + \rho^{-1} \boldsymbol{W} = \boldsymbol{0}. \tag{21}$$

On Γ_b the adoption of the homogeneous Dirichlet condition $\boldsymbol{U} = \boldsymbol{0}$ would imply to resolve the boundary layer, which is not of interest for the present application. Therefore, we replace it with an impenetrability condition coupled with an empirical relation that accounts for the friction with the bottom surface. We also assume, for the sake of simplicity, that h is constant. We have then

$$\begin{cases} \boldsymbol{U}\cdot\boldsymbol{N} = 0 \Rightarrow w = 0 \\ \nu \dfrac{\partial \boldsymbol{u}}{\partial z} = \dfrac{|\boldsymbol{u}|\boldsymbol{u}}{C_D^2}, \end{cases} \qquad \text{on } \Gamma_b, \tag{22}$$

where C_D is the so-called Chezy coefficient (see for instance [11]).

Moreover, we operate on the kinematic condition (5), to get an expression that is more convenient for the discretization. Namely, we integrate the continuity equation (6) along the vertical direction and we exploit (5) and (22) to obtain to the so-called *integral condition for the free surface*, that is

$$\frac{\partial \eta}{\partial t} + \nabla\boldsymbol{\cdot}\int_{-h}^{\eta} \boldsymbol{u}\,dz = 0.$$

To summarize, we consider the following system of equations, at each time $t \in (0,T)$,

$$\begin{cases} \dfrac{D\boldsymbol{u}}{Dt} - \dfrac{\partial}{\partial z}\left(\nu \dfrac{\partial \boldsymbol{u}}{\partial z}\right) + g\boldsymbol{\nabla}\eta + \boldsymbol{\nabla}\lambda + \boldsymbol{\nabla} q = \boldsymbol{0}, \\ \dfrac{Dw}{Dt} - \dfrac{\partial}{\partial z}\left(\nu \dfrac{\partial w}{\partial z}\right) + \dfrac{\partial q}{\partial z} = 0, \\ \nabla\boldsymbol{\cdot}\boldsymbol{u} + \dfrac{\partial w}{\partial z} = 0, \end{cases} \qquad \text{in } \Omega(t), \tag{23}$$

$$\begin{cases} \dfrac{\partial \eta}{\partial t} + \nabla\boldsymbol{\cdot}\displaystyle\int_{-h}^{\eta} \boldsymbol{u}\,dz = 0, \\ \lambda(\eta - \Psi) = 0, \quad \lambda \geq 0, \quad \eta - \Psi \leq 0 \end{cases} \qquad \text{in } \omega(t), \tag{24}$$

provided with boundary conditions (7), (22) and (21).

2 Time discretization and weak formulation

Time discretization is performed via characteristics. We subdivide the time interval $[0,T]$ into N sub-intervals of width Δt and denote with the subscript n the approximation at $t = t^n$ of the various time-dependent quantities. For the sake of simplicity, yet with no loss of generality, we are assuming a constant time step.

Let $\mathbf{X}^n = \mathbf{X}(\mathbf{x}, t^{n+1}; t^n)$ be the position at time t^n of the material point that is located in $\mathbf{x}$ at time t^{n+1}. The method of characteristics consists in performing the following approximation,

$$\frac{D\boldsymbol{U}}{Dt}(\mathbf{x}, t^{n+1}) \simeq \frac{\boldsymbol{U}(\mathbf{x}, t^{n+1}) - \boldsymbol{U}(\mathbf{X}^n, t^n))}{\Delta t}, \tag{25}$$

where $\mathbf{X}^n$ is computed by solving the following time backward differential problem for each $\mathbf{x} \in \Omega(t)$,

$$\begin{cases} \dfrac{d\boldsymbol{X}}{d\tau}(\mathbf{x}, t^{n+1}; t^{n+1} - \tau) = -\boldsymbol{U}(\mathbf{X}(\mathbf{x}, t^{n+1}; t^{n+1} - \tau), t^{n+1} - \tau), \quad \tau \in (0, \Delta t), \\ \boldsymbol{X}(\mathbf{x}, t^{n+1}; t^{n+1}) = \mathbf{x}. \end{cases}$$

More details on this technique may be found in [4] or in [12]. The time discretised equations now read

$$\begin{array}{ll} \dfrac{\boldsymbol{u}^{n+1} - \boldsymbol{u}^n(\mathbf{X}^n)}{\Delta t} - \nu \dfrac{\partial \boldsymbol{u}^{n+1}}{\partial z} + g\boldsymbol{\nabla}\eta^{n+1} + \boldsymbol{\nabla}\lambda^{n+1} + \boldsymbol{\nabla} q^{n+1} = \mathbf{0}, & \\ \dfrac{w^{n+1} - w^n(\mathbf{X}^n)}{\Delta t} - \nu \dfrac{\partial w^{n+1}}{\partial z} + \dfrac{\partial q^{n+1}}{\partial z} = 0, & \text{in } \Omega^{n+1}, \\ \nabla\boldsymbol{\cdot}\boldsymbol{u}^{n+1} + \dfrac{\partial w^{n+1}}{\partial z} = 0, & \\ \dfrac{\eta^{n+1} - \eta^n}{\Delta t} + \nabla\boldsymbol{\cdot}\displaystyle\int_{-h}^{\eta^{\triangle}} \boldsymbol{u}^{n+1}\, dz = 0, & \text{in } \omega, \\ \lambda^{n+1}(\eta^{n+1} - \Psi^{n+1}) = 0, \quad \lambda \geq 0, \quad \eta^{n+1} - \Psi^{n+1} \leq 0, & \end{array} \tag{26}$$

where quantities at time t^n are assumed to be known from the previous computation for $n = 1, 2, \ldots$, and given by the initial data for $n = 0$ and $\eta^{\triangle}$ is a suitable approximation of η^{n+1}, introduced to avoid solving a non-linear problem.

From now on and for the sake of notation we omit the superscript $n+1$ for the unknown quantities at the n-th time step. Furthermore, we choose $\eta^{\triangle} = \eta^n$, which introduces a truncation error of the first order in time. Another possibility, leading to a second order error, would be to set $\eta^{\triangle} = 2\eta^n - \eta^{n-1}$, using linear extrapolation.

2.1 Weak formulation setting

We have reduced our time dependent problem to a sequence of (coupled in time) elliptic problems (26), for which we now seek a convenient weak formulation.

At every time step t^{n+1}, we set $\Omega = \omega \times (-h, \eta^n)$ and we look for a solution $\boldsymbol{U} = (\boldsymbol{u}, w)^T \in \mathcal{U} = \mathcal{U}_{\boldsymbol{u}} \otimes \mathcal{U}_w$ where

$$\mathcal{U}_{\boldsymbol{u}} = \left\{ \boldsymbol{v} \in \left[L^2(\omega)\right]^2 : \nabla\boldsymbol{\cdot}\boldsymbol{v} \in L^2(\omega), \boldsymbol{v} \cdot \boldsymbol{n} = 0 \right\} \times H^1(-h, \eta^n(x, y)),$$

$$\mathcal{U}_w = L^2(\omega) \times \left\{ \phi \in H^1(-h, \eta^n(x, y)), \phi = 0 \text{ on } z = -h \right\}.$$

Here $L^2(\Omega)$ denotes the usual Sobolev space of square integrable functions on the domain Ω, and $H^1(\Omega)$ the space of $L^2(\Omega)$ functions whose partial derivatives still belong to $L^2(\Omega)$ [13].

We seek w in $\mathcal{U}_w$ rather than the usual $H^1(\Omega)$ space, since our treatment of the Cauchy stress tensor allows a weaker regularity in the x and y coordinates.

Furthermore, we seek the hydrodynamic pressure q in $L^2(\Omega)$, and η and λ in $L^2(\omega)$.

Let $\boldsymbol{V} = (\boldsymbol{v}, z)^T \in \mathcal{U}$ be a test function for the velocity. We define the following bilinear forms,

$$a(\boldsymbol{U},\boldsymbol{V}) = \int_\omega \int_{-h}^{\eta^n(x,y)} \frac{1}{\Delta t}\boldsymbol{U}\cdot\boldsymbol{V}\mathrm{d}\omega\mathrm{d}z + \nu \int_\omega \int_{-h}^{\eta^n(x,y)} \frac{\partial \boldsymbol{U}}{\partial z}\cdot\frac{\partial \boldsymbol{V}}{\partial z}\mathrm{d}\omega\mathrm{d}z,$$

$$d(\boldsymbol{U},q) = -\int_\omega \int_{-h}^{\eta^n(x,y)} q\nabla\boldsymbol{\cdot}\boldsymbol{U}\mathrm{d}\omega\mathrm{d}z,$$

$$b(\boldsymbol{U},\lambda) = -\int_\omega \lambda\left(\nabla\boldsymbol{\cdot}\int_{-h}^{\eta^n(x,y)} \boldsymbol{u}dz\right)\mathrm{d}\omega.$$

The bilinear form $b(\boldsymbol{U},\lambda)$ results from the fact that

$$\int_\omega \int_{-h}^{\eta^n(x,y)} \widetilde{\boldsymbol{\nabla}}\lambda\cdot\boldsymbol{U}\mathrm{d}\omega\mathrm{d}z = \int_\omega \int_{-h}^{\eta^n(x,y)} \boldsymbol{\nabla}\lambda\cdot\boldsymbol{u}\mathrm{d}\omega\mathrm{d}z = \int_\omega \boldsymbol{\nabla}\lambda\cdot\left(\int_{-h}^{\eta^n(x,y)} \boldsymbol{u}\mathrm{d}z\right)\mathrm{d}\omega =$$

$$\underbrace{\int_{\partial\omega}\lambda\,\boldsymbol{n}\cdot\int_{-h}^{\eta^n(x,y)}\boldsymbol{u}\mathrm{d}z}_{0,\boldsymbol{u}\cdot\boldsymbol{n}=0} - \int_\omega \lambda\left(\nabla\boldsymbol{\cdot}\int_{-h}^{\eta^n(x,y)} \boldsymbol{u}dz\right)\mathrm{d}\omega = -\int_\omega \lambda\left(\nabla\boldsymbol{\cdot}\int_{-h}^{\eta^n(x,y)} \boldsymbol{u}dz\right)\mathrm{d}\omega = b(\boldsymbol{U},\lambda),$$

while the same procedure leads to

$$\int_\omega \int_{-h}^{\eta^n(x,y)} g\widetilde{\boldsymbol{\nabla}}\eta\cdot\boldsymbol{U}\mathrm{d}\omega\mathrm{d}z = g\ b(\boldsymbol{U},\eta).$$

In conclusion, the weak formulation of the momentum equation is: find $\boldsymbol{U}\in\mathcal{U}$ and $q\in L^2(\Omega)$ such that

$$a(\boldsymbol{U},\boldsymbol{V}) + g\ b(\boldsymbol{V},\eta) + b(\boldsymbol{V},\lambda) + d(\boldsymbol{V},q) = F(\boldsymbol{V}), \quad \forall\boldsymbol{V}\in\mathcal{U}$$

where $F(\boldsymbol{V})$ is the linear functional that takes in account the boundary conditions on the free surface and on the bottom,

$$F(\boldsymbol{V}) = \int_{\Gamma_s} \rho^{-1}\boldsymbol{W}\cdot\boldsymbol{V}\mathrm{d}\gamma_s - \int_\omega \frac{|\boldsymbol{u}^n|\boldsymbol{u}^n}{C_D^2}\cdot\boldsymbol{v}\mathrm{d}\omega + \frac{1}{\Delta t}\int_\omega \int_{-h}^{\eta^n(x,y)} \boldsymbol{U}^n\cdot\boldsymbol{V}\mathrm{d}\omega\mathrm{d}z$$

As for the free surface equation, we first rewrite it more conveniently as

$$\eta = \eta^n + \Delta t\nabla\boldsymbol{\cdot}\int_{-h}^{\eta^n}\boldsymbol{u}dz. \tag{27}$$

We introduce a test function χ in $L^2(\omega)$ and denote by $(\cdot,\cdot)_\omega$ the scalar product in $L^2(\omega)$. With this notation, the weak formulation of (27) is given by

$$(\eta,\chi)_\omega = (\eta^n,\chi)_\omega + \int_\omega \Delta t\left(\nabla\boldsymbol{\cdot}\int_{-h}^{\eta^n}\boldsymbol{u}\mathrm{d}z\right)\chi\mathrm{d}\omega = (\eta^n,\chi)_\omega - \Delta t\ b(\boldsymbol{U},\chi), \tag{28}$$

for all $\chi \in L^2(\omega)$.

We point out that the equation for the free surface (both in its strong form (27) and in the weak form (28)) gives in fact an explicit dependence of η with $\boldsymbol{U}$, i.e. we may formally write $\eta = \eta(\boldsymbol{U})$. This fact will be exploited in the next section.

Finally, we derive the weak formulation for the buoyancy constraint by inserting (27) into the unilateral constraint $\eta \leq \Psi$, obtaining

$$\int_\omega \left(\nabla \cdot \int_{-h}^{\eta^n} \boldsymbol{u} dz \right) \chi \mathrm{d}\omega \leq \left(\frac{\Psi - \eta^n}{\Delta t}, \chi \right)_\omega ,$$

for all $\chi \in L^2(\omega)$, that is $-b(\boldsymbol{U}, \chi) = G(\chi)$, having set $G(\chi) = \left(\frac{\Psi - \eta^n}{\Delta t}, \chi \right)_\omega$.

We are now in the position to state the following

Weak formulation 1. *Find $\boldsymbol{U} \in \mathcal{U}, \eta, \lambda \in L^2(\omega)$ and $q \in L^2(\Omega)$ such that*

$$\begin{aligned}
&a(\boldsymbol{U}, \boldsymbol{V}) + g\, b(\boldsymbol{V}, \eta) + b(\boldsymbol{V}, \lambda) + d(\boldsymbol{V}, q) = F(\boldsymbol{V}), && \forall \boldsymbol{V} \in \mathcal{U} \\
&d(\boldsymbol{U}, r) = 0, && \forall r \in L^2(\Omega) \\
&(\eta, \chi)_\omega = (\eta^n, \chi)_\omega - \Delta t\, b(\boldsymbol{U}, \chi), && \forall \chi \in L^2(\omega) \\
&-b(\boldsymbol{U}, \chi) \leq G(\chi) && \forall \chi \in L^2(\omega)
\end{aligned}$$

with $\lambda \geq 0$ such that $(\lambda, \eta - \Psi)_\omega = 0$.

3 Iterative solution by Uzawa method

We may interpret weak formulation 1 as the optimality conditions of a constrained optimization problem. We exploit this fact to solve our problem via duality techniques by applying the Uzawa algorithm to the dual problem. We follow closely the theoretical setting illustrated in [14, Chapter V].

To this aim, let us go back to the pressure splitting (17). We collect all pressure terms apart from λ into a single term p, i.e. we set $\rho p = \rho q + \rho g(\eta - z) + \Pi_a$. The pressure splitting becomes $\Pi = \rho p + \rho \lambda$, and the weak formulation is rewritten as

Weak formulation 2. *find $\boldsymbol{U}^* \in \mathcal{U}, \eta^*, \lambda^* \in L^2(\omega), p^* \in L^2(\Omega)$ such that*

$$\begin{aligned}
&a(\boldsymbol{U}^*, \boldsymbol{V}) + b(\boldsymbol{V}, \lambda^*) + d(\boldsymbol{V}, p^*) = F(\boldsymbol{V}), && \forall \boldsymbol{V} \in \mathcal{U} \\
&d(\boldsymbol{U}^*, r) = 0, && \forall r \in L^2(\Omega) \\
&-b(\boldsymbol{U}^*, \chi) \leq G(\chi) && \forall \chi \in L^2(\omega)
\end{aligned}$$

with $\lambda^* \geq 0$ such that $(\lambda^*, \eta^* - \Psi)_\omega = 0$ and $(\eta^*, \chi)_\omega = (\eta^{*,n}, \chi)_\omega - \Delta t\, b(\boldsymbol{U}^*, \chi)$ $\forall \chi \in L^2(\omega)$.

Exploiting relation (27), we can read this formulation as the KKT conditions for the saddle point of the Lagrangian functional

$$L(\boldsymbol{U}, p, \lambda) = J(\boldsymbol{U}) + d(\boldsymbol{U}, p) + \int_\omega \lambda \left(\frac{\eta(\boldsymbol{U}) - \Psi}{\Delta t} \right) \mathrm{d}\omega \tag{29}$$

where $J(\boldsymbol{U}) = \frac{1}{2}a(\boldsymbol{U}, \boldsymbol{U}) + F(\boldsymbol{U})$. The Lagrangian functional L is associated to the following constrained optimization problem,

$$\begin{aligned} &\text{find } \boldsymbol{U}^* : J(\boldsymbol{U}^*) = \min_{\boldsymbol{U} \in \mathcal{U}} J(\boldsymbol{U}) \\ &\text{subject to } \nabla \cdot \boldsymbol{U}^* = 0, \\ &\qquad \text{and } \frac{\eta(\boldsymbol{U}^*) - \Psi}{\Delta t} \leq 0. \end{aligned} \tag{30}$$

We recognize λ as the Lagrange multiplier for the floating constraint, in the very same way as p is the Lagrange multiplier for incompressibility constraint. From here on we refer to problem (30) as *primal problem.*

Note that the incompressibility constraint is an equality constraint, therefore the corresponding Lagrange multiplier p can be chosen in $L^2(\Omega)$. On the contrary, the floating constraint is an inequality constraint, hence the corresponding Lagrange multiplier has to be non-negative.
It is possible to show (Prop. 1.1 [14]) that the primal problem (30) is equivalent to the so-called *minimax problem*:

$$find\ (\boldsymbol{U}^*, p^*, \lambda^*) : L(\boldsymbol{U}^*, p^*, \lambda^*) = \inf_{\boldsymbol{U} \in \mathcal{U}} \sup_{p \in L^2(\Omega)} \sup_{\lambda \in \Lambda} L(\boldsymbol{U}, p, \lambda) \tag{31}$$

Note that the minimax point is not necessarily a saddle point [1]. The crucial point is that if one can show that L has a saddle point in $(\boldsymbol{U}^*, p^*, \lambda^*)$, then it holds that (prop. 1.2 [14])

$$\inf_{\boldsymbol{U} \in \mathcal{U}} \sup_{p \in L^2(\Omega)} \sup_{\lambda \in \Lambda} L(\boldsymbol{U}, p, \lambda) = L(\boldsymbol{U}^*, p^*, \lambda^*) = \sup_{\lambda \in \Lambda} \sup_{p \in L^2(\Omega)} \inf_{\boldsymbol{U} \in \mathcal{U}} L(\boldsymbol{U}, p, \lambda) \tag{32}$$

For our Lagrangian functional, the existence of a saddle point is guaranteed by the application of the Ky-Fan and Sion Theorem [14, Theorem 3.1].

We define the *dual function* as

$$w(\lambda) = \sup_{p \in L^2(\Omega)} \inf_{\boldsymbol{U} \in \mathcal{U}} L(\boldsymbol{U}, p, \lambda)$$

and the *dual problem* as

$$find\ \lambda^* : w(\lambda^*) = \sup_{\lambda \in \Lambda} w(\lambda). \tag{33}$$

[1] A saddle point for L is defined as $(\widehat{\boldsymbol{U}}, \hat{p}, \hat{\lambda}) : L(\widehat{\boldsymbol{U}}, p, \lambda) \leq L(\widehat{\boldsymbol{U}}, \hat{p}, \hat{\lambda}) \leq L(\boldsymbol{U}, \hat{p}, \hat{\lambda})$

Then, thanks to the *strong duality theorem* (prop. 1.4 [14]), if $(\boldsymbol{U}^*, \lambda^*, p^*)$ is a saddle point for L, then $\boldsymbol{U}^*$ is solution of the primal problem and λ^* is solution of the dual problem. This means that we can obtain the solution of (30) by solving the dual problem instead, which is much more appealing since the only constraint is here the positivity of λ, which can be treated easily by a numerical algorithm.

The dual function w associates to any feasible λ the solution of the corresponding Navier-Stokes problem with free surface and boat pressure profile λ. Of course, it is impossible to have an explicit expression of such a function. Therefore, we resort to the well known *Uzawa algorithm* [15], which may be stated in the following form,

Algorithm 1 (Uzawa Method)**.** *given two tolerances $\epsilon_1 > 0$ and $\epsilon_2 > 0$ and starting from $\lambda_{(0)} = 0$, for $k = 0, 1, \ldots$ compute $\eta_{(k)} \in L^2(\omega)$, $\boldsymbol{U}_{(k)} \in \mathcal{U}$ and $q_{(k)} \in L^2(\Omega)$ such that*

$$\begin{aligned}
&a(\boldsymbol{U}_{(k)}, \boldsymbol{V}) + b(\boldsymbol{V}, \lambda_{(k)}) + g\, b(\boldsymbol{V}, \eta_{(k)}) + d(\boldsymbol{V}, q_{(k)}) = F(\boldsymbol{V}), && \forall \boldsymbol{V} \in \mathcal{U}\\
&d(\boldsymbol{U}_{(k)}, r) = 0, && \forall r \in L^2(\Omega)\\
&\left(\eta_{(k)}, \chi\right)_\omega = (\eta^n, \chi)_\omega - \Delta t\; b(\boldsymbol{U}_{(k)}, \chi), && \forall \chi \in L^2(\omega),
\end{aligned}$$

and update λ according to the rule

$$\lambda_{(k+1)} = \max\left(\lambda_{(k)} + \alpha_{(k)} \frac{\eta_{(k)} - \Psi}{\Delta t}, 0\right), \tag{34}$$

$\alpha_{(k)}$ being a parameter suitably chosen to assure convergence. The sequence is stopped when $|\left(\lambda_{(k)}, \eta_{(k)} - \Psi\right)_\omega| \leq \epsilon_1$ and $\Psi - \eta_{(k)} > -\epsilon_2$. We use the last computed quantities as the approximation of $\boldsymbol{U}^*$, p^*, η^* and λ^* at the given time step. Here, $F(\boldsymbol{V})$ accounts for all the known terms and we have expanded back the pressure term p to put into evidence the role of η and the hydrodynamic correction q.

The convergence of the Uzawa method in Sobolev spaces is ensured by Theorem 3.3 in [14], which states that the sequence $\{(\boldsymbol{U}_{(k)}, p_{(k)}),\ k = 0, 1, \ldots\}$ converges strongly to the (unique) solution of the primal problem, and any cluster point of the sequence $\{\lambda_{(k)},\ k = 0, 1, \ldots\}$ is a solution for the dual problem.

4 Finite element implementation

We will now introduce the finite element scheme we have adopted for the space discretization, We also describe a fractional step method for the solution of the resulting algebraic system that allows an efficient implementation of the Uzawa iterations just presented. For a more detailed description of the finite element scheme and fractional step methods for free surface flows see [4, 16].

The domain is subdivided along the z-axis into Nl layers and a triangular grid for the xy plane is replicated at the midpoint of each layer, leading in fact to a prismatic grid.

We indicate with Nt and Ne the number of triangles and the number of edges in the xy plane mesh, respectively. The horizontal velocity is approximated combining the lowest order Raviart-Thomas elements ($\mathbb{RT}_0$) in the xy plane with the $\mathbb{P}_1$ elements along the vertical direction, that is the approximated velocity $\boldsymbol{u}_h$ may be expressed as

$$\boldsymbol{u}_h(x,y,z) = \sum_{j=1}^{Nl}\sum_{e=1}^{Ne} U_{j,e}\boldsymbol{\tau}_e(x,y)\varphi_j(z), \tag{35}$$

where $U_{j,e}$ is the generic degree of freedom associated to the lateral face defined by the edge e and the layer j, while $\{\boldsymbol{\tau}_e,\, j = 1,\ldots,N_l\}$ and $\{\varphi_j,\, j = 1,\ldots,Ne\}$ are the canonical basis of $\mathbb{RT}_0(\omega)$ and $\mathbb{P}_1(-h,\eta^n)$, respectively. For the definition of this finite element spaces and their approximation properties the interested reader may refer to [17, 18]. As for the vertical velocity w, we use piecewise constant elements ($\mathbb{P}_0$) in the horizontal plane and linear finite elements in the z direction, that is the approximated vertical velocity may be expressed as

$$w_h(x,y,z) = \sum_{j=1}^{Nl}\sum_{i=1}^{Nt} w_{j,i}\chi_i(x,y)\varphi_j(z), \tag{36}$$

where $\{\chi_i,\, i = 1,\ldots,Nt\}$ is the canonical basis for the finite element space $\mathbb{P}_0(\omega)$, and $w_{j,i}$ the degree of freedom associated to triangle i and layer j. Finally the elevation and the Lagrange multiplier are approximated using piecewise constant functions, i.e. the approximating functions η_h and λ_h read

$$\eta_h(x,y) = \sum_{i=1}^{Nt}\eta_i\chi_i(x,y), \qquad \lambda_h(x,y) = \sum_{i=1}^{Nt}\lambda_i\chi_i(x,y), \tag{37}$$

while the hydrodynamic pressure is approximated with piecewise constant functions on each prism,

$$q_h(x,y,z) = \sum_{j=1}^{Nl}\sum_{i=1}^{Nt} q_{j,i}\chi_i(x,y)\xi_j(z), \tag{38}$$

$\{\xi_j,\, j = 1,\ldots,Nl\}$ being the basis of the $\mathbb{P}_0(-h,\eta^n)$ finite element space built on the vertical grid defined by the layers. Here λ_i, η_i and $q_{j,i}$ indicate the degrees of freedom for the Lagrange multiplier, the elevation, and the hydrodynamic pressure, respectively. More details about this particular discretization may be found in [4]. Here we just mention that even if the domain shape changes in the z direction, since η^n is indeed a function of (x,y) varying at each time step, the actual implementation is done on a fixed grid whose vertical extension is sufficient to accommodate all the expected variations of the free surface, and the "dry" elements are not taken into account in the construction of the final linear system.

If we consider now the discretization of a generic iteration k of Algorithm 1 we obtain an algebraic system of the form:

$$\begin{bmatrix} \mathrm{A} & \mathrm{D}^T \\ \mathrm{D} & 0 \end{bmatrix} \begin{bmatrix} \boldsymbol{V} \\ \boldsymbol{Q} \end{bmatrix} = \begin{bmatrix} \widehat{\boldsymbol{F}}_{(k)} \\ \boldsymbol{0} \end{bmatrix}, \tag{39}$$

where $\boldsymbol{V} = (\boldsymbol{U}_{(k)}, \boldsymbol{H}_{(k)}, \boldsymbol{W}_{(k)})^T$ is the vector collecting the degrees of freedom for the horizontal components of the velocity, the elevation and the vertical velocity respectively, $\boldsymbol{Q} = \boldsymbol{Q}_{(k)}$ indicates the vector of the degrees of freedom for the hydrodynamic pressure and $\widehat{\boldsymbol{F}}_{(k)} = (\widehat{\boldsymbol{F}}_{\boldsymbol{u},(k)}, \widehat{\boldsymbol{F}}_{\eta}, \widehat{\boldsymbol{F}}_{w})^T$ accounts for boundary conditions, the terms arising from the time derivative and the Lagrange multiplier, that is

$$\boldsymbol{F}_{\boldsymbol{u},(k)} = \frac{1}{\Delta t}\boldsymbol{U}^n(\boldsymbol{X}) - \mathrm{B}^T\boldsymbol{\Lambda}_{(k)}, \quad \boldsymbol{F}_\eta = \frac{1}{\Delta t}\boldsymbol{H}^n, \quad \boldsymbol{F}_w = \frac{1}{\Delta t}\boldsymbol{W}^n(\boldsymbol{X}).$$

We have indicated with $\boldsymbol{\Lambda}_{(k)}$ the vector of discrete Lagrange multipliers at the k-th Uzawa iteration, and with B^T the algebraic operator associated to the bilinear form $b(\boldsymbol{V}, \lambda)$. The term $(\boldsymbol{X})$ indicates that the corresponding degrees of freedom have been computed by extrapolation at the foot of the characteristics, in according to the adopted discretization of the time derivative.

The matrices A and D can be further expanded as follows

$$\mathrm{A} = \begin{bmatrix} \frac{1}{\Delta t}\mathrm{M_u} + \mathrm{K_u} & g\mathrm{B}^T & 0 \\ \mathrm{B} & \frac{1}{\Delta t}\mathrm{M}_\eta & 0 \\ 0 & 0 & \frac{1}{\Delta t}\mathrm{M_w} + \mathrm{K_w} \end{bmatrix}, \quad \mathrm{D}^T = \begin{bmatrix} \mathrm{D}_{xy}^T \\ 0 \\ \mathrm{D}_z^T \end{bmatrix},$$

where $\mathrm{M}_{\boldsymbol{u}}$, M_η, M_w are the mass matrices for the corresponding components of the unknowns, $\mathrm{K}_{\boldsymbol{u}}$, K_η and K_w are the corresponding stiffness matrices, and finally D is the discrete $3D$ divergence operator. In this algebraic setting, if we indicate with $\boldsymbol{\Psi}$ the vector containing the value of Ψ at each triangle barycenter, the convergence test becomes

$$||\boldsymbol{\Lambda}.^*(\boldsymbol{H}_{(k)} - \boldsymbol{\Psi})|| \leq \epsilon_1 \quad \text{and} \ \min(\boldsymbol{\Psi} - \boldsymbol{H}_{(k)}) > -\epsilon_2, \tag{40}$$

where $.^*$ indicates the element-by-element product, and the update of the multiplier

$$\boldsymbol{\Lambda}_{(k+1)} = \max\left(\boldsymbol{\Lambda}_{(k)} + \frac{\alpha_{(k)}}{\Delta t}\left(\boldsymbol{H}_{(k)} - \boldsymbol{\Psi}\right), \boldsymbol{0}\right). \tag{41}$$

We may note that only $F_{\boldsymbol{u}}$ depends on the Uzawa iteration k, an important fact that will be exploited in the following fractional step splitting.

4.1 A fractional step scheme

System (39) implies a solution for all the unknowns of the problem at each Uzawa iteration, a rather costly operation for realistic problems where the number of degrees of freedom may be rather large.

In [16] some fractional step schemes have been proposed to ease the computations. We will now show that one of those schemes, which is akin to the well known Chorin-Temam splitting for Navier-Stokes problems, will also allow an efficient implementation of the Uzawa iterations.

Let us consider the updating rule (34) for λ in more detail. It states that the only quantity needed for the Uzawa iterations is η. This means that all the other variables computed at each Uzawa iteration are unnecessary, and it would be possible to reduce greatly the computation time if one can find a fractional step scheme where the updating of η is less costly.

With a fractional step scheme we split the solution of Navier Stokes equations into an hydrostatic step and an hydrodynamic correction. The hydrostatic step computes the elevation η and an approximation of velocity, while the hydrodynamic correction computes the hydrodynamic pressure q and modifies the value of $\boldsymbol{U}$, but does not affect η. Therefore, the hydrostatic step is the only one required for the Uzawa iterations, with great saving of computational time.

The procedure is then described by the following algorithm.

Algorithm 2 (Fractional step scheme)**.** *At each time step the computations involve four steps.*

Hydrostatic step and Uzawa iterations

Starting from a given $\boldsymbol{\Lambda}_{(0)}$*, for* $k = 0, 1, \ldots$ *we solve*

$$\left\{ \begin{aligned} \left(\frac{1}{\Delta t}\mathrm{M}_{\boldsymbol{u}} + \mathrm{K}_{\boldsymbol{u}}\right)\widetilde{\boldsymbol{U}}_{(k)} + g\mathrm{B}^T\boldsymbol{H}_{(k)} &= \frac{1}{\Delta t}\mathrm{M}_{\boldsymbol{u}}\boldsymbol{U}^n(\boldsymbol{X}) - \mathrm{B}^T\boldsymbol{\Lambda}_{(k)}, \\ \mathrm{B}\widetilde{\boldsymbol{U}}_{(k)} + \frac{1}{\Delta t}\mathrm{M}_\eta\boldsymbol{H}_{(k)} &= \frac{1}{\Delta t}\mathrm{M}_\eta\boldsymbol{H}^n, \end{aligned} \right. \tag{42}$$

and update $\boldsymbol{\Lambda}$ *according to (41) until the stopping criteria (40) is reached. We indicate with* $\widetilde{\boldsymbol{U}}$*,* $\boldsymbol{H}$*, and* $\boldsymbol{\Lambda}$ *the converged degrees of freedom for the horizontal velocity, elevation and multiplier.*

Intermediate vertical velocity component evaluation

We compute $\widetilde{\boldsymbol{W}}$ *by solving the system*

$$\left(\frac{1}{\Delta t}\mathrm{M}_w + \mathrm{K}_w\right)\widetilde{\boldsymbol{W}} = \frac{1}{\Delta t}\mathrm{M}_w\boldsymbol{W}^n(\boldsymbol{X}).$$

Hydrodynamic pressure computation

$$-\Delta t \left[\mathrm{D_{xy}} \mathrm{M}_u^{-1} \mathrm{D_{xy}}^T + \mathrm{D_z} \mathrm{M}_w^{-1} \mathrm{D_z}^T\right] \boldsymbol{Q} = -\left(\mathrm{D_{xy}} \widetilde{\boldsymbol{U}} + \mathrm{D_z} \widetilde{\boldsymbol{W}}\right). \tag{43}$$

Hydrodynamic correction on the velocity components

$$\begin{cases} \boldsymbol{U} = \widetilde{\boldsymbol{U}} - \Delta t \mathrm{M}_u^{-1} \mathrm{D}_{xy}^T \boldsymbol{Q}, \\ \boldsymbol{W} = \widetilde{\boldsymbol{W}} - \Delta t \mathrm{M}_w^{-1} \mathrm{D}_z^T \boldsymbol{Q}. \end{cases} \tag{44}$$

As was already stated, the hydrodynamic correction step does not affect the computation of the elevation η. Moreover, thanks to the special structure of the mass and stiffness matrices, with some algebraic manipulations it is possible to modify the hydrostatic step to eliminate the computation of the velocity $\widetilde{\boldsymbol{U}}_{(k)}$ and solve just for $\boldsymbol{H}_{(k)}$. The horizontal velocity degrees of freedom are then calculated only after the convergence of the Uzawa iterations. This technique saves further computational time for the Uzawa iterations.

5 Numerical Results

5.1 Fluid-Body Coupling

The main goal of our simulations is to describe the dynamic of a rowing scull, taking into account its secondary motions as pitching and sinking. For a description of the problem the reader may refer to [3, 19].

Since in this work we are concerned mainly in describing the method rather than in the applications, we consider here a simplified dynamics for the boat. It is determined fully by the external forces acting on the scull given by the weight of the boat and the pressure λ.

The position at time t of the boat is described by six degrees of freedom (the x, y and z coordinates of a given point of the boat and three angles that define its angular position, e.g. roll ϕ, yaw ψ and pitch θ), and the complete dynamic is tracked with six equations, one for each degree of freedom.

Let us focus on the sinking (similar calculations can be performed for each secondary motion). Denoting with $z(t)$ the vertical position of the bottom of the scull, the corresponding Cauchy problem reads:

$$\begin{cases} \ddot{z} = -g + \frac{\boldsymbol{F}_z(\lambda,t)}{m} \\ z(0) = z_0 \\ \dot{z}(0) = 0 \end{cases} \tag{45}$$

where z_0 is the initial position of the scull and $\boldsymbol{F}_z(\lambda, t)$ is the vertical projection of the pressure force $\boldsymbol{F}$ performed by the boat, calculated as $\boldsymbol{F}(\lambda, t) = \int \lambda \mathrm{d}\Psi(t)$, that can be computed numerically.

At each time step, given $z(t)$ and $\dot{z}(t) = v(t)$, one calculates:

1. the scull position, i.e. the constraint $\Psi(t)$;
2. $\lambda(t)$, by solving the Navier-Stokes equations;
3. the overall acceleration at time t, $\ddot{z}(t) = a(t) = -g + \frac{\boldsymbol{F}(\lambda,t)}{m}$.

Next one performs time integration for (45). Notice that it is not possible to use any implicit method with reasonable computational cost, since it is not possible to know $F(t+\Delta t)$ before $z(t+\Delta t)$. We consider two different integration schemes

1. *Quasi Explicit Euler*:

$$\begin{cases} v(t+\Delta t) = v(t) + a(t)\Delta t \\ z(t+\Delta t) = z(t) + v(t)\Delta t + \frac{1}{2}a(t)\Delta t^2 \end{cases} \tag{46}$$

2. *Quasi Newmark*: in this case we use an approximation of $a(t+\Delta t)$, $a^*(t+\Delta t) = 2a(t) - a(t-\Delta t)$, and then write:

$$\begin{cases} v(t+\Delta t) = v(t) + \left(\dfrac{a(t) + a^*(t+\Delta t)}{2}\right)\Delta t \\ \\ z(t+\Delta t) = z(t) + v(t)\Delta t + \dfrac{1}{2}\left(\dfrac{a(t) + a^*(t+\Delta t)}{2}\right)\Delta t^2 \end{cases} \tag{47}$$

5.2 Sinking motion test

In this section we perform several sinking motion experiments, as described in equation (45). We want to test if the algorithm is able to predict correctly the stationary regime and the stationary pressure on the scull; we also want to assess the accuracy of the several time integration schemes we proposed. We can easily check whether the results are reasonable, since we can exactly calculate the final values for z and $\boldsymbol{F}_z$ by Archimedes' Principle.

The tests are performed with a boat whose dimensions are $8 \times 0.8 \times 0.6$ m (length $\times$ width $\times$ height), with weight 400 kg, over a $20 \times 12 \times 36$ m grid. We define the z coordinate in (45) as the non-wet portion of the boat, and we set the initial position of the scull z_0 as $z_0 = 0.6$, so that at the initial time the boat is out of the water, touching the free surface $\eta(0)$ only at its bottom. By Archimedes' Principle, the steady value for z is 0.32 m.

Results are shown in figure 1. First of all, we notice that a reasonable time step is $\Delta t \approx 0.02$ s; the results obtained with bigger time steps are affected by oscillations (or do not converge at all, e.g. if $\Delta t = 0.1$ s).

The different schemes reasonably converge to the same solution for $\Delta t \approx 0.02$, as shown in figure 2, and all the stationary regimes adequately agrees with the predicted one. However, the Quasi Explicit Euler method overestimates the undershooting, whereas the Quasi Newmark appears to be the most physically reasonable, because of the rebound predicted at $t \approx 0.5$ s (see figure 2-right).

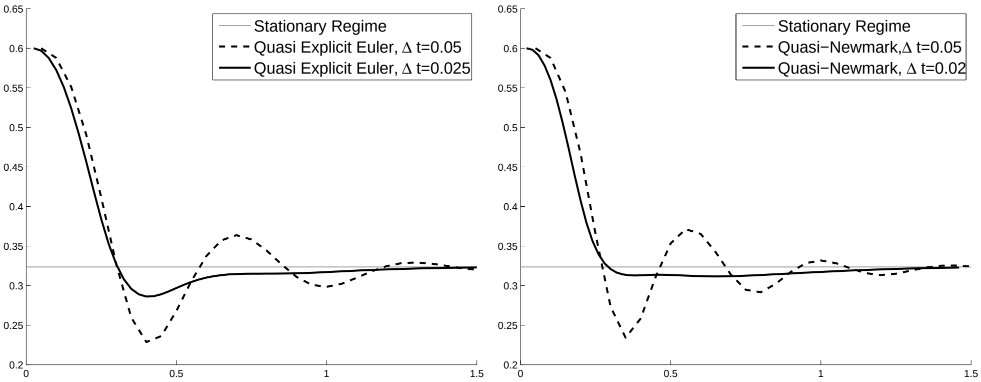

Figure 1: Comparison for different Δt: Quasi Explicit Euler (left) and Quasi Newmark (right)

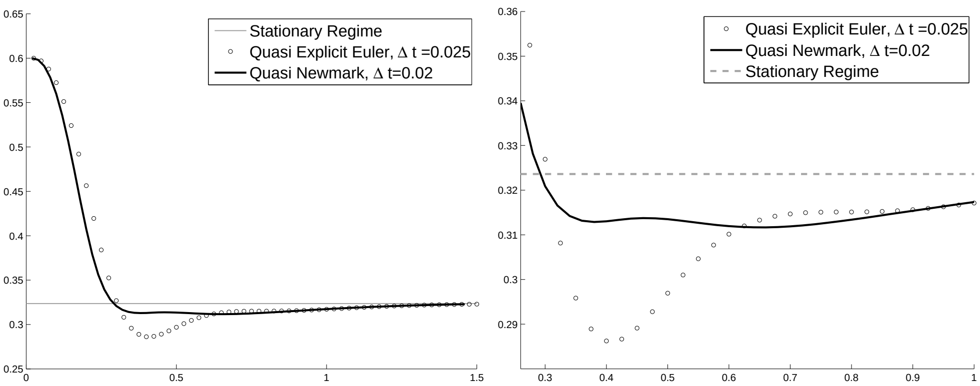

Figure 2: Comparison of different methods: whole dynamic (left) and zoom on the undershooting (right)

Another interesting comparison is between the hydrostatic and hydrodynamic simulations: in general, the hydrostatic approximation seems to be quite inaccurate, since it shows wider and persisting oscillations, see figure 3.

6 Conclusions

In this work we have proposed a novel approach to handle the buoyancy of boats, and in general floating objects by enforcing an inequality constraint over the elevation of the free surface η. Despite the fact that this approach is limited to situations where the wave do not overturn, many problems can be addressed with this method. It represent an alternative to volume of fluid or level-set methods.

We have presented an implementation of the imposition of the constraints which is rather efficient and it exploits the algebraic structure resulting from the

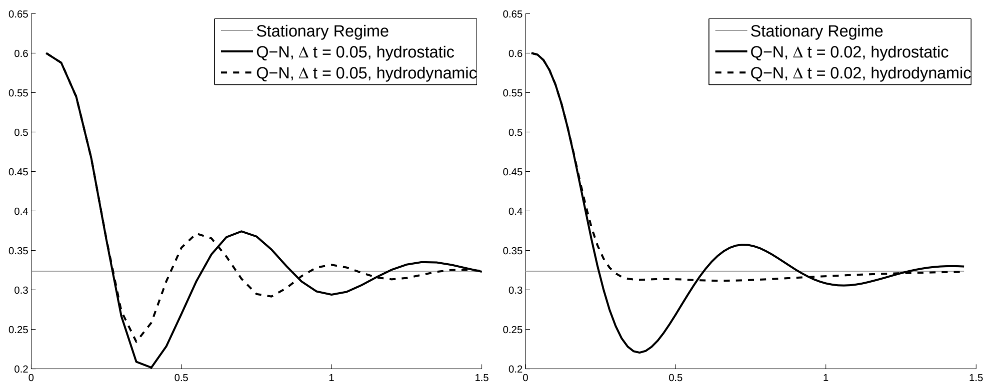

Figure 3: Comparison between hydrostatic and hydrodynamic solutions for different time steps

choice of a particular finite element representation.

We have demonstrated the effectiveness of the method on some simple cases, since this work is more focused on the methodological aspects than applications. Yet, some preliminary results on the hydrostatic system, presented in [5], show how the method is effective to solve the fluid-structure interaction problems, where the position of the floating object is governed by its own dynamics. In this context, the Lagrange multiplier provide information on the force acting on the body.

There are still some open problems which are subject to current investigations. The first is the necessity of replacing the slip condition on the boat surface with a relation accounting for the viscous effects. For slender body it is possible to foresee the interaction with a simplified model for the boundary layer able to characterize the term that has been generically indicated with $\boldsymbol{W}$ in Section 1.

The second concerns the optimal choice for the parameter $\alpha_{(k)}$. So far we have used some heuristics derived from the theory of unconstrained optimization. A more in depth analysis is in principle possible, leading to optimal convergence rates.

The simplified form for the Cauchy stress tensor has helped to reduce the computational effort, since it has allowed to adopt rather simple finite elements (we mention in passing that the scheme can be easily implemented on parallel architectures). However, the general technique for the imposition of the constraint does not depend on this choice, even if so far, at the best of our knowledge, there have been no attempts in this direction.

7 Acknowledgments

This work has been prompted by a collaboration with Filippi Lido srl, a manufacturer of competition rowing boats, which we gratefully acknowledge. The last three authors acknowledge also the support of the Italian Ministry of Research, through PRIN 2007 and PRIN 2008 grants. A thank is also due to Michele Altieri for his work on the C++ version of the code and to Andrea Mola.

References

[1] R. Azcueta. Computation of turbulent free-surface flows around ships and floating bodies. *Ship Technology Research*, 49(2):46–69, 2002.

[2] N. Parolini and A. Quarteroni. Mathematical models and numerical simulations for the America's Cup. *Comp. Meth. Appl. Mech. Engng.*, 194(9-11):1001–1026, 2005.

[3] L. Formaggia, E. Miglio, A. Mola, and A. Montano. A model for the dynamics of rowing boats. *Internat. J. Numer. Methods Fluids*, 61(2):119–143, 2009.

[4] E. Miglio, A. Quarteroni, and F. Saleri. Finite element approximation of quasi-3D shallow water equations. *Comp. Meth. Appl. Mech. Engng.*, 174(3-4):355–369, 1999.

[5] L. Formaggia, E. Miglio, A. Mola, and A. Scotti. Numerical simulation of the dynamics of boats by a variational inequality approach. In *Variational analysis and aerospace engineering*, volume 33 of *Springer Optim. Appl.*, pages 213–227. Springer, New York, 2009.

[6] J. Serrin. Mathematical principles of classical fluid mechanics. *Handbuch der Physik*, 8(1):125, 1959.

[7] C. D. Levermore and M. Sammartino. A shallow water model with eddy viscosity for basins with varying bottom topography. *Nonlinearity*, 14(6):1493, 2001.

[8] S. Ferrari and F. Saleri. A new two-dimensional shallow water model including pressure effects and slow varying bottom topography. *M2AN*, 38(2):211–234, 2004.

[9] G.L. Mellor and A.F. Blumberg. Modeling vertical and horizontal diffusivities with the sigma coordinate system. *Monthly Weather Review*, 113(8):1379–1383, 1985.

[10] E. Wolanski, T. Asaeda, A. Tanaka, and E. Deleersnijder. Three-dimensional island wakes in the field, laboratory experiments and numerical models. *Continental Shelf Research*, 16(11):1437 – 1452, 1996.

[11] W. L. Wood. *Introduction to numerical methods for water resources.* Oxford Science Publications. The Clarendon Press Oxford University Press, New York, 1993.

[12] K. Boukir, Y. Maday, B. Métivet, and E. Razafindrakoto. A high-order characteristics/finite element method for the incompressible Navier-Stokes equations. *Internat. J. Numer. Methods Fluids*, 25(12):1421–1454, 1997.

[13] R. A. Adams. *Sobolev spaces*. Academic Press, New York-London, 1975. Pure and Applied Mathematics, Vol. 65.

[14] J. Cea. *Lectures on Optimizazion - theory and algorithms*. Tata Institute of Fundamental Research, Bombay, 1978.

[15] R. Glowinski and P. Le Tallec. *Augmented Lagrangian and operator-splitting methods in nonlinear mechanics*, volume 9 of *Studies in Applied Mathematics*. SIAM, Philadelphia, 1989.

[16] P. Causin, E. Miglio, and F. Saleri. Algebraic factorizations for 3D non-hydrostatic free surface flows. *Comput. Vis. Sci.*, 5(2):85–94, 2002.

[17] F. Brezzi and M. Fortin. *Mixed and hybrid finite element methods*, volume 15 of *Springer Series in Computational Mathematics*. Springer-Verlag, New York, 1991.

[18] A. Quarteroni and A. Valli. *Numerical approximation of partial differential equations*, volume 23 of *Springer Series in Computational Mathematics*. Springer-Verlag, Berlin, 1994.

[19] L. Formaggia, A. Mola, N. Parolini, and M. Pischiutta. A three-dimensional model for the dynamics and hydrodynamics of rowing boats. *Proceedings of the Institution of Mechanical Engineers, Part P: Journal of Sports Engineering and Technology*, 224(1):51–61, 2010.

MOX Technical Reports, last issues

Dipartimento di Matematica "F. Brioschi",
Politecnico di Milano, Via Bonardi 9 - 20133 Milano (Italy)

24/2010 Lorenzo Tamellini, Luca Formaggia, Edie Miglio, Anna Scotti:
An Uzawa iterative scheme for the simulation of floating boats

23/2010 Joakim Baeck, Fabio Nobile, Lorenzo Tamellini, Raul Tempone:
Stochastic Spectral Galerkin and collocation methods for PDEs with random coefficients: a numerical comparison

22/2010 Carlo D'Angelo, Paolo Zunino:
Numerical approximation with Nitsche's coupling of transient Stokes'/Darcy's flow problems applied to hemodynamics

21/2010 Niccolo' Grieco, Francesca Ieva, Anna Maria paganoni:
Provider Profiling Using Mixed Effects Models on a Case Study concerning STEMI Patients

20/2010 Fabio Nobile, Alfio Quarteroni, Ricardo Ruiz Baier:
Numerical solution of an active strain formulation for the electro-mechanical activity in the heart

19/2010 Loredana Gaudio, Alfio Quarteroni:
hN-adaptive spectral element discretization of optimal control problems for environmental applications

18/2010 Paola F. Antonietti, Nur Aiman Fadel, Marco Verani:
Modelling and numerical simulation of the polymeric extrusion process in textile products

17/2010 Alessandra Guglielmi, Francesca Ieva, Anna Maria Paganoni, Fabrizio Ruggeri:
A Bayesian random-effects model for survival probabilities after acute myocardial infarction

16/2010 Luca Formaggia, Anna Scotti:
Positivity and conservation properties of some integration schemes for mass action kinetics

15/2010 Alfio Quarteroni, Luca Formaggia:
Domain Decomposition (DD) methods